

A DSC investigation of the crystallization kinetics of polyoxymethylene

C. J. G. Plummer* and H.-H. Kausch

Ecole Polytechnique Fédérale de Lausanne, CH-1015 Lausanne, Switzerland

Abstract

The large spherulite size, heterogeneous nucleation and constant spherulite growth rate of POM suggests a straightforward two dimensional Avrami analysis, with two adjustable parameters, $t_0(T)$ and $K(T)$, to be appropriate to thin samples in the DSC. For $T > 147$ °C, spherulite densities inferred from results for the rate parameter $K(T)$ and microscopical measurements of spherulite growth rates are consistent with observed spherulite sizes. The $K(T)$ values may also be used to model non-isothermal crystallization in the same temperature range ($dT/dt < 10$ K/minute). Whilst $K(T)$ shows little dependence on molecular weight, samples containing 30 wt% TPU crystallize more slowly owing to a reduced nucleation density.

Introduction

Differential scanning calorimetry (DSC) has been used here to characterize and compare the crystallization kinetics of various grades of polyoxymethylene (POM), based on the Avrami equation

$$X(t) = 1 - \exp(-Kt^n) \quad \dots (1),$$

where $X(t)$ is the degree of crystallinity (normalized with respect to the degree of crystallinity at $t = \infty$), n is the Avrami exponent and K is a rate factor [1]. For small t , equation (1) may be written $X(t) \sim Kt^n$. In the case of heterogeneous nucleation, for two- and three-dimensional spherulitic growth we have then,

$$X(t) = N\pi G^2 t^2 \quad \text{and} \quad X(t) = \frac{N4\pi G^3 t^3}{3} \quad \dots (2)$$

respectively, where N is the nucleation density and G is the radial spherulitic growth rate (assumed to be independent of t). Thus for simple two-dimensional spherulitic growth, $n = 2$ and $K = N\pi G^2$.

More general forms of equation (1) have been advanced to take into account effects such as thermal nucleation and secondary crystallization, which are either known to occur in given systems or which have been invoked to account for deviations from equation (1) and/or non-integral values of n [1]. Care must be taken however, since as the number of adjustable parameters increases, 'goodness of fit' to the data is no longer a sufficient criterion for acceptance of a given model, and any such choice must be corroborated by independent

*Corresponding author

observations. In the present case, for example, it was found that excellent fits could be obtained to isothermal crystallization curves by assuming, heterogeneous nucleation, three-dimensional spherulitic growth and using the Hillier model for secondary crystallization to account for deviations from equation (1) at long times [2]. Here $X = X_1 + X_2$ where

$$X_1 = X_0 (1 - \exp(-K_1 t^3))$$

$$X_2 = (1 - X_0) K_2 \int_0^t (1 - \exp(-K_1 \tau^3)) \exp(-K_2(t - \tau)) d\tau.$$

In Figure (1) the fit was obtained with $K_1 = 9 \times 10^{-4} \text{ s}^{-3}$, $K_2 = 1.2 \times 10^{-1} \text{ s}^{-1}$ and $X_0 = 0.75$. For three-dimensional spherulite growth $K_1 = N4\pi G^3/3$, and at 145°C , $G \sim 3 \times 10^{-5} \text{ ms}^{-1}$, so that the implied nucleation density $N \sim 8 \times 10^9 \text{ m}^{-3}$ which suggests a final spherulite diameter of the order of $600 \mu\text{m}$. Since the sample weighed only 3 mg, with a thickness of a few tens of μm , the above three-dimensional analysis is clearly inconsistent.

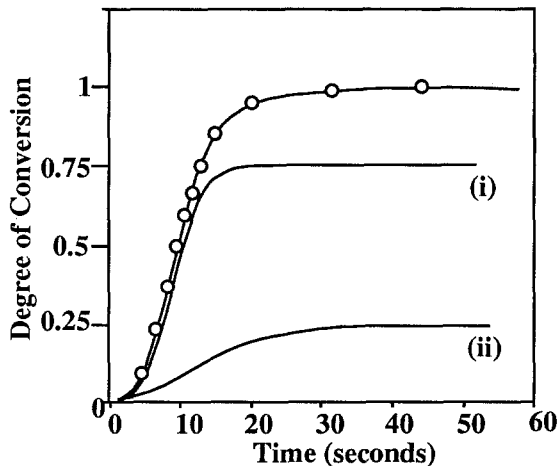


Figure 1. Fit of Hillier's model with $n = 3$ to isothermal crystallization data for POM, $M_w = 41,000$ and $T_c = 145^\circ\text{C}$ (curve (i) primary crystallization, curve (ii) secondary crystallization).

Examination of microtomed slices of DSC crystallized samples suggests POM spherulites have diameters of several hundred μm , so a more realistic approach is to use two-dimensional analysis, assuming that the sample may be idealized as a continuous thin film.

Experimental

Pure ex-reactor POM of molecular weights 35×10^3 , 41×10^3 and 66×10^3 was available in powder form. Measurements were carried out under nitrogen using the Perkin Elmer DSC 7. Approximately 3 mg of powder was spread evenly on the bottom of the DSC capsule. For the isothermal measurements, the samples were melted in the DSC at 200°C for 1 minute, and cooled at 200 K/minute to the required crystallization temperature. The sample was examined subsequent to each measurement by optical microscopy to check for uniform wetting and to assess the spherulite size. For comparison, measurements were carried out on a commercial 30 wt% thermoplastic polyurethane (TPU) filled grade with $M_w = 66 \times 10^3$. In this case $10 \mu\text{m}$

slices were microtomed from injection mouldings (in which the rubber phase was well dispersed) and cut to fit the sample holder. The DSC was calibrated using an indium standard, and baselines were obtained by extrapolation of the linear portion of the crystallization curves (at times well beyond the crystallization peak). The correction for the temperature-lag in non-isothermal measurements was estimated to be 0.25 dT/dt from measurements of melting peak shifts as a function of heating rate in 3 mg samples of POM isothermally crystallized at 150°C .

Analysis

Optical hot stage microscopy suggests (i) that the nucleation may be considered heterogeneous (N constant), (ii) that G is constant in time, (iii) that there is a certain time delay t_0 prior to the onset of nucleation. Since t_0 is difficult to measure unambiguously it is treated here as an adjustable parameter. For two dimensional spherulite growth, and for $t > t_0$, equation (1) becomes

$$X(t) = 1 - \exp(-K(t - t_0)^2) \quad \dots (3).$$

Examples of experimental data for crystallization temperatures between 145 and 155°C fitted to equation (3) are shown in Figure (2) for $M_w = 41 \times 10^3$ and 66×10^3 along with the experimental values for K and t_0 . The data are given in reduced form; $X(t)$ is plotted against $(t - t_0)/(t_{1/2} - t_0)$ where $t_{1/2}$ is the time at which $X = 0.5$.

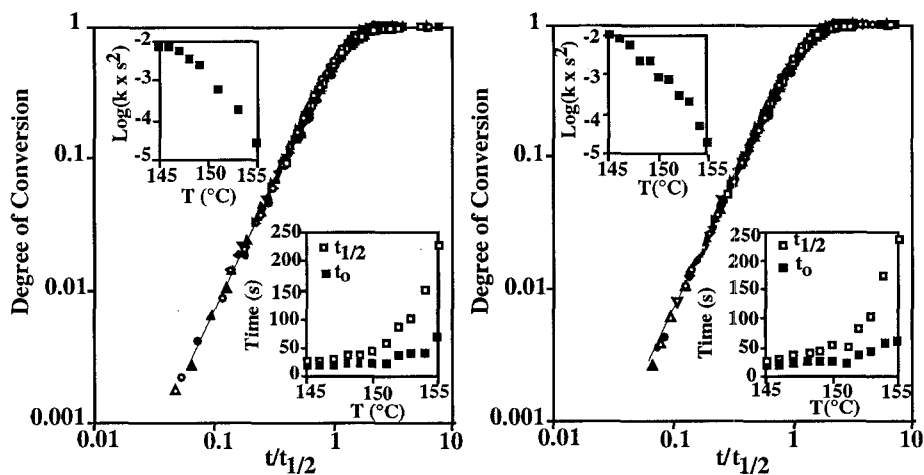


Figure (2). Experimental data for crystallization temperatures between 145 and 155°C fitted to equation (3) for $M_w = 41 \times 10^3$ and 66×10^3 along with the experimental values for K and t_0 .

To test the usefulness of this two-parameter description of spherulite growth, it was used to predict the form of the crystallization curves during cooling at constant dT/dt , assuming crystallization to start at $T_0 = T_m - t_i (dT/dt)$ where t_i is a (dynamic) incubation time which will be assumed to be zero unless stated otherwise, so that T_0 is the temperature of the melt (200°C). Following [3], the thermal history is modelled as a series of isothermal crystallizations of duration Δt , such that T diminishes by an amount ΔT after completion of each step. Consider a two-stage crystallization such that the sample is maintained for time Δt at T_1 and the

temperature then lowered to T_2 . After Δt at T_1 , for Avrami type crystallization with exponent n the degree of crystallization is

$$X(\Delta t) = 1 - \exp(-K(T_1)\Delta t^n)$$

After Δt at $T_2 < T_1$ (a total time of $2\Delta t$), we have

$$X(2\Delta t) = 1 - \exp(-K(T_2)(\Delta t + t')^n) \quad \dots (4).$$

where t' is the time at which a degree of crystallinity X_1 would have been reached if crystallization had started at T_2 instead of T_1 . The inclusion of t' follows since X must be continuous at Δt , whence

$$t' = \left(\frac{\Delta t K(T_1)}{K(T_2)} \right)^{1/n}$$

By substituting this expression back into equation (4) and generalizing to n steps, we obtain

$$X(n\Delta t) = 1 - \exp(- \left\{ \sum_{i=1}^n K(T_i)^{1/n} \Delta t \right\}^n),$$

and in the continuous limit, letting $T = T_0 - \alpha t$,

$$X(t) = 1 - \exp(- \left\{ \int_0^t K(T_0 - \alpha\tau)^{1/n} d\tau \right\}^n)$$

or

$$X(T) = 1 - \exp(- \left\{ \alpha^{-1} \int_{T_0}^T K(\Theta)^{1/n} d\Theta \right\}^n) \quad \dots (5),$$

where T_0 is the temperature at which crystallization starts. The integral term in equation (5) is equivalent to the cooling function in the Ozawa equation [3]. An attempt was made to estimate t_i by assuming that nucleation occurred when the condition

$$\int_0^{t_i} \frac{\tau}{t_0(\tau)} d\tau = 1 \quad \dots (6)$$

was satisfied, where $\tau = (T_m - T) \cdot \alpha^{-1}$ and $T_m = 200$ °C. $t_0(T)$ was estimated by interpolating the experimental values obtained from isothermal measurements.

In the present case $K(T)$ is taken to be $N\pi G(T)^2$, where from fits of Hoffman's expressions for regime III growth ($T < 160$ °C) to experimental G data [4,5]

$$\log G(T) = \log G_{III} = 7.7 - 1.96 \times 10^5 / T\Delta T - 30,000 / 2.3RT \quad \dots (7),$$

($\Delta T \sim T - T_{m0}$ and $T_{m0} = 200$ °C). Taking $N = 1.9 \times 10^7 \text{ m}^{-2}$ gives $K(T)$, which is compared with the isothermal data for different grades in Figure (3). Figure (3) suggests use of equation (7) to be justifiable for $T > 147$ °C; below this temperature $K(T)$ falls off more rapidly with

temperature than predicted for constant N . It was also found that for $\alpha \leq 10$ K/min, use of $T_0 = T_m - \alpha t_i$, where t_i is estimated from equation (6) made little difference to the final result. Similarly, departures from equation (7) above 160 °C owing to the onset of regime II crystallization [4,5] were insignificant for $\alpha \geq 0.1$ K/min, which was the lowest cooling rate used experimentally.

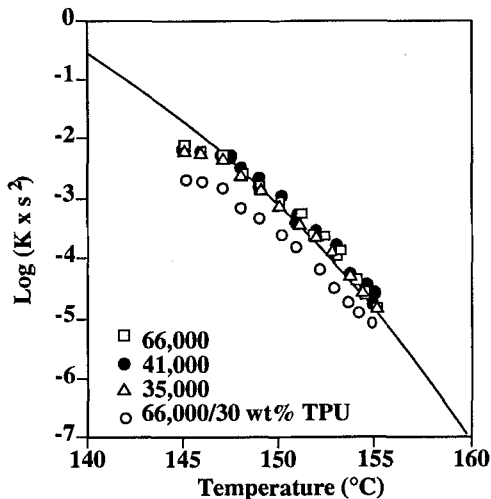


Figure (3) Comparison of $K(T)$ as inferred from temperature dependence of G and constant $N = 1.9 \times 10^7 \text{ m}^{-2}$, and experimental data for POM, $M_w = 41 \times 10^3$.

Examples of predicted and measured cooling curves are shown in Figure (4) for $M_w = 41 \times 10^3$ and for $10 \geq \alpha \geq 0.1$, using $G(T)$ from equation (7) and

$$\frac{dH(T)}{dt} = A \frac{d}{dT} \left(1 - \exp\left(-\pi N \left\{ \alpha^{-1} \int_{T_0}^T G(T) dT \right\}^2 \right) \right),$$

where A is $\alpha \Delta H$ (ΔH is the total enthalpy change). That reasonable agreement is obtained reflects the fact that crystallization occurs at $T > 147$ °C for the rates shown.

At cooling rates greater than approximately 10 K/min, the predicted and measured crystallization curves begin to differ in shape. This is difficult to interpret in view of the lack of experimental data (the temperature regime corresponding to $dT/dt > 10$ K/minute is inaccessible to the isothermal technique), the break-down of equation (7) at low T , and uncertainties regarding the degree of temperature lag and t_i , as will be discussed in the next paragraph. It is possible that at T where the crystallization times may be similar to the incubation times, effects relating to the nucleation rate can no longer be ignored. Indeed, the deviation of the isothermal $K(T)$ values from those predicted by equation (7) at low T may already reflect this - G may be sufficiently rapid at these temperatures for potential nucleation sites to be swallowed up by spherulites nucleated after relatively short times, lowering the effective value of N [1]. Finally, as the cooling rate continues to rise, and the degree of undercooling increases, $G(T)$ should eventually begin to fall owing to transport effects, and homogeneous (thermal) nucleation may intervene. Very fine microstructures are obtained for example when samples melted in the DSC

are removed and immediately quenched to room temperature in a water bath. Unfortunately this regime is not easily accessible to the present experimental techniques.

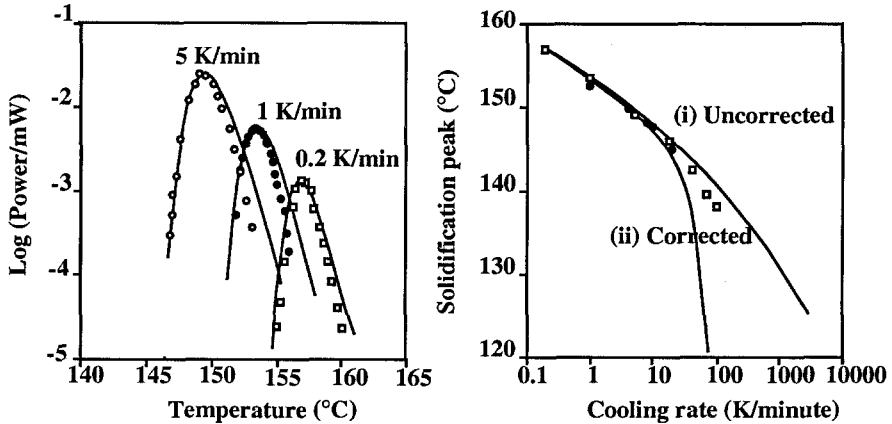


Figure (4). (a) Predicted and measured crystallization curves for different cooling rates for POM, $M_w = 41 \times 10^3$; (b) Predicted and measured crystallization peak as a function of cooling rate with (i) no correction for t_0 and (ii) corrected for t_0 using equation (4).

Remaining within the experimentally accessible temperature range, at low T , the predicted position of the crystallization peak may be significantly affected by the estimates of t_i . A comparison of peak positions obtained (i) by ignoring the effect of t_i (that is, taking T_0 equal to 200 °C) and (ii) by incorporating t_i as estimated using linear extrapolation of experimental values of $t_0(T)$ for $T < 150$ °C to obtain $t_0(T)$ for $T < 145$ °C, along with the experimental data points is shown in Figure 4(b). Assuming the corrections to the data for temperature lag to be accurate, this suggests there is little basis for incorporating the t_0 determined from the fits to the isothermal data in modelling the non-isothermal behaviour in this regime, and indeed it is likely that the isothermal data are themselves significantly affected by temperature lag where crystallization times are short, making it difficult to interpret the measured t_0 .

Discussion

The simple two-dimensional analysis of DSC data for thin samples in the range 145 to 155 °C given above provides a working description of both isothermal and non-isothermal crystallization kinetics of POM in this same temperature range. The corresponding G values obtained by optical microscopy are independent of M_w within the margin of experimental error [5]. They reflect well the $K(T)$ variation for $M_w = 35 \times 10^3$, 41×10^3 and 66×10^3 for $T > 147$ °C as shown in Figure (5) so that within the framework of the model N appears to be not only independent of T but also of M_w , consistent with the assumption of heterogeneous nucleation. Individual values of N show considerable scatter (reflected by that of K). Given a mean value of N of $1.9 \times 10^7 \text{ m}^{-2}$, we anticipate a centre-to-centre spherulite separation of the order 350 μm (assuming hexagonal close packing), consistent with direct observation of the samples. A uniformly thick sample covering the whole of the bottom of the DSC capsule (an area of about $25 \times 10^{-6} \text{ m}^2$) should therefore represent approximately 500 spherulites. However, whilst this should represent a sufficiently large statistical sample, thickness variations, incomplete wetting of the capsule and the presence of voids may considerably decrease the effective number of spherulites, increasing the amount of scatter.

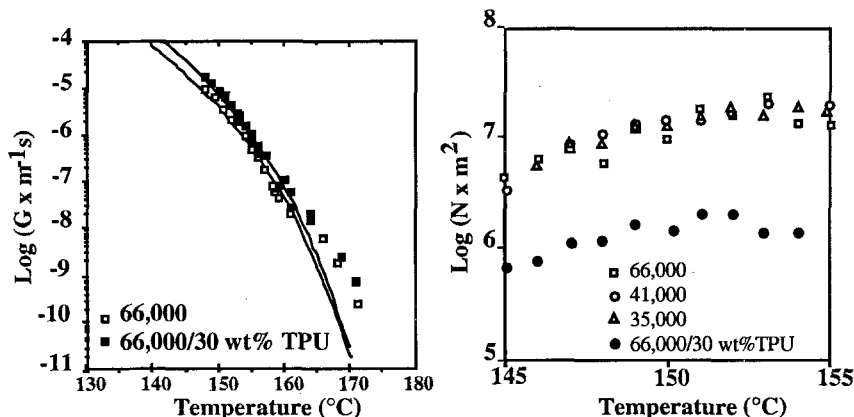


Figure (5): (a) Radial spherulite growth rates in POM and POM/30 wt% TPU; (b) Nucleation densities for all grades investigated.

To test this dependence further we have examined the behaviour of a POM/30 wt% TPU blend. The K values obtained for this polymer were given in Figure (3). Measurements of G are shown in Figure 5(a) and estimates of the N are shown in Figure 5(b). Since G is found to be a factor of approximately 1.5 higher than in the unfilled POM grades, on the basis of the model, the lower K values, and hence the slower crystallization kinetics should reflect a reduced nucleation density. We have compared the mean centre-to-centre spherulite separation as estimated from $1.5 N^{-1/2}$, with values measured from optical microscopic investigations of the crystallized films. The results are shown in Table I, indicating reasonable agreement for the highest temperatures, but poorer agreement at 145°C .

	Predicted spherulite separation (μm)			Measured spherulite separation (μm)		
	66K	35K	66K/TPU	66K	35K	66K/TPU
145 $^{\circ}\text{C}$	740	760	1900	400	450	1200
150 $^{\circ}\text{C}$	350	360	900	400	320	1000
155 $^{\circ}\text{C}$	335	339	900	395	330	975

Table I: Calculated and measured spherulite centre-to-centre separations

Conclusion

In the temperature regime $T > 147^{\circ}\text{C}$, the present results indicate two-dimensional Avrami analysis, with two adjustable parameters, $t_0(T)$ and $K(T)$, to provide a working description of crystallization in the DSC for samples whose thickness is much less than the spherulite diameters. The analysis appears consistent with microscopical measurements of spherulite growth rates and the spherulite diameters of the isothermally crystallized samples, although further and more detailed measurements are required to confirm this. Use of solution cast films on a suitable substrate may avoid uncertainties associated with sample homogeneity and wetting. We also envisage more sophisticated treatment of DSC data, taking into account changes in heat capacity and temperature lag [6,7] coupled with systematic measurement of spherulite sizes in the samples. Finally, dilatometric measurements of crystallization rates on bulk samples would determine the extent to which results for three-dimensional spherulite growth are consistent with those obtained here. As far as the present results are concerned,

whilst $K(T)$ shows little dependence on molecular weight for pure POM, samples containing 30 wt% TPU crystallize more slowly owing to a reduced nucleation density (this in spite of a slightly higher spherulite growth rate).

Acknowledgements

The financial support of DuPont de Nemours Ltd. is gratefully acknowledged.

References

1. Wunderlich, B. (1976), *Macromolecular Physics*, Vol. 2, Academic Press, New York.
2. Hillier, I.H. (1965), *J. Poly. Sci. Part A* 3, 3067.
3. Ozawa, T. (1971), *Polymer* 12, 150.
4. Hofmann, J.D., *Polymer* 24, 3 (1983).
5. Plummer, C.J.G., Menu, P., Cudré-Mauroux, N., Kausch, H.-H., Submitted to *J. Appl. Poly. Sci.*.
6. Eder, M., Wlochowicz, A. (1983), *Polymer* 24, 1593.
7. Hay, J.N., Mills, P.J. (1982), *Polymer* 23, 1380.

Accepted November 8, 1993 C